RSC Advances

ROYAL SOCIETY OF CHEMISTRY

www.rsc.org/advances

Oxidation of SO_2 and NO by epoxy groups on graphene oxides: The role of the hydroxyl group

Wanglai Cen, [1, 2] Meiling Hou, [1] Jie Liu, [3] Shandong Yuan, [4] Yongjun Liu, [1, 2] Yinghao Chu[1, 2*]

1. College of Architecture and Environment, Sichuan University, Chengdu 610065, P.R. China;

2. National Engineering Research Center for Flue Gas Desulfurization, Chengdu 610065, P.R. China;

3. Department of Environment Engineering, Chengdu University of Information Technology, Chengdu 610025, P. R. China.

4. Institute of New Energy and Low Carbon Technology, Sichuan University, Chengdu 610065, P.R. China.

Corresponding author: Associate Prof. Yinghao Chu (chuyinghao@scu.edu.cn)

Abstract

Simultaneous catalytic removal of SO_2 and NO_x at low temperature (< 150 °C) has long been recognized as a challenge for the treatment of coal-burned flue gases. Density functional theory corrected with dispersion was used to investigate the potential of graphene oxides (GOs) for the catalytic oxidation of SO_2 and NO_x. It is found that both the SO_2 and NO_x can be oxidized by epoxy groups of GO nearly at room temperature. The hydroxyl groups on the GO surface enhance the adsorption and oxidation of SO_2, and of NO as well, but in quite different ways. For the case of SO_2, the promotion is derived from the formation of charge transfer channels, which are fabricated by the hydroxyl group, the adsorbed SO_2 and the epoxy group. The promotion is enhanced by the introduction of more hydroxyl groups as more charge transfer channels are formed. However, for NO, the hydroxyl group leads to a strong N-C covalent interaction between the adsorbed NO molecules and the GO surface, through which the NO is activated and oxidized with a much lower barrier. These results provide a mechanistic explanation of the low temperature catalytic oxidation of SO_2 and NO by carbon materials and insights into designing new carbon-based catalysts.

Key words: First principles, hydrogen bond, catalytic oxidation, desulfuration, denitration

1. Introduction

Simultaneously catalytic removal of sulfur dioxide (SO_2) and nitric oxide (NO) from the flue gases emitted by burnt fossil fuels is still a challenge, both in scientific research and industrial applications.[1-3] Recently, it was found that SO_2 can be catalytically oxidized by graphene oxides (GOs) to SO_3 experimentally at room temperature.[4] It motivated our theoretical investigations on the mechanism of highly efficient catalytic oxidation of SO_2 by GOs, and the potential application in the catalytic removal of NO.

Acutally, carbon materials, for example, granular activated carbon or activated carbon fibers, have long been studied for the catalytic removal of SO_2 at low temperature (20-150°C).[5-8] In the reaction, SO_2 is oxidized to form SO_3, which in turn is hydrated to sulfuric acid in the presence of water. The oxidation of SO_2 to SO_3 is supposed to be the rate-determining step[9] and can be improved by introduction of surface oxygen groups (C–O complexes).[17-19] Due to the complex geometric and chemical structures of actual carbon catalysts, the dependence of the adsorption and oxidation of SO_2 on surface C-O complexes is still an open question.

According to Long et al.[4], the hydroxyl and epoxy groups on a GO surface are responsible for the efficient catalytic oxidation of SO_2 by GOs at room temperature. It spotlights the confusing desulfurization mechanism of carbon materials at the atomic level. Based on ab initio calculations, Yang and Yang[9] proposed that catalytic oxidation of SO_2 occurs on the edge of the microstructure of carbon materials. The initial step is the adsorption and oxidation of SO_2 by surface oxygen species. The hydroxyl group was also indentified to play a key role in the chemical reaction catalyzed by GO.[10] These results indicate that both epoxy and hydroxyl groups

might have important effects on the adsorption and catalytic oxidation of SO_2.

The catalytic removal of NO by carbon materials at room temperature has also been reported, dating back to more than two decades.[11-16] In the reaction, NO is catalytically oxidized to NO_2, which is further converted to HNO_3 in the presence of water. However, understanding of the catalytic mechanism is much less than that for SO_2. Practical applications are limited so far by the unsatisfactory state of knowledge. Very recently, Tang and Cao[17] reported that the hydroxyl group enhances the adsorption of NO on the GO surface. Details for the oxidation of NO were not included.

In a typical catalytic oxidation loop, the active oxygen species on the surface of catalysts are consumed, and must be regenerated dynamically. Radovic and coauthors[18,19] found that surface oxygen species can be formed by O atom spillover after O_2 dissociation on the edge sites of graphene. It could be enhanced by N-doping[20-22] and As decoration[23]. Our previous theoretical work[24] investigated the adsorption of SO_2 on different GOs, and the feasibility for oxidation. In the present study, we focus on two points: (1) the mechanism and capacity for the promotion of the hydroxyl group to the oxidation of SO_2 by carbon materials; (2) whether the promotion could be spread to the oxidation of NO. The oxidation of CO is investigated as well for comparison. Single atomic layer graphene functionalized with combinations of hydroxyl and epoxy groups is used as the model carbon material.

2. Models and methods

2.1 Computational models

Single atomic layer graphene with a rectangular boundary (12.78×14.76 Å, denoted as GP)

was used as the substrate material, as depicted in Figure 1. A vacuum region of 20 Å was added perpendicular to the graphene plane to minimize the interaction between the two nearby layers.[17] Single O atom was added at a bridge site to form an epoxy group, denoted by OGP, as shown in Figure 1a. A hydroxyl group (OH) was added to OGP to fabricate HO_OGP1 (Figure 1b) or HO_OGP2 (Figure 1c). The two different bridge sites of the epoxy group, referring the OH were used due to the different sizes of SO_2, NO and CO molecules. The optimized adsorption configuration of SO_2 on the OGP surface was denoted by SO_2/OGP. Other adsorption configurations were denoted along the same lines.

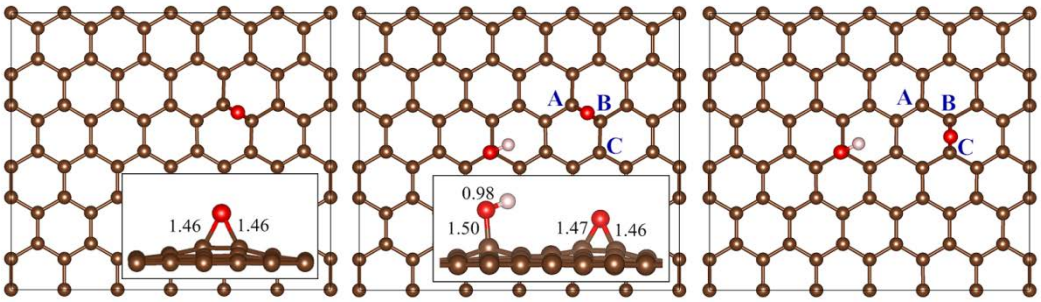

Figure 1 Relaxed geometric structures of (a) OGP, (b) HO_OGP1 and (c) HO_OGP2. The brown, red and gray balls stand for carbon, oxygen and hydrogen atoms, respectively. Three carbon atoms are labeled as A, B and C. The O atom of the epoxy is located at the bridge site A-B for HO_OGP1 and the bridge site B-C for HO_OGP2. All lengths in the insets of (a) and (b) are given in Å.

2.2 Computational methods

All the density functional theory (DFT) calculations were carried out with the code VASP5.2,[25,26] using the generalized gradient approximation with a Perdew-Burke-Ernzerhof (PBE) exchange and correlation functional.[27] A plane-wave basis set with cut-off energy 400 eV was employed within the framework of the projector augmented-wave (PAW) method.[28,29] The

Brillouin zone was sampled with a 3×3×1 k-points mesh, generated by the Monkhorst-Pack algorithm. Gaussian smearing was used, with a smearing width 0.2 eV. The D2 method of Grimme[30] was used to describe the van der Waals (vdW) correction with the default parameters. Actually, the D2 method only depicts the dispersion part of the vdW force empirically. There exist more complex non-local vdW functionals[31], however, it is not clear how to make a choice[32]. We therefore tested at least the optB88-vdW functional, which was found to be in excellent agreement with experimental data for organic molecules adsorption on graphene[33]. We showed (Table S1) that the adsorption energies from optB88-vdW are albeit systematically lower than that from PBE-D2, however, the variation trend was unchanged. We therefore used PBE-D2 in our work.

The atoms on the boundary were frozen in all directions. All the remaining atoms were relaxed until the maximum Hellman-Feynman force was less than 0.02 eV/Å. Spin polarization and the zero-point energy correction were not included. All the above parameters were sufficient to ensure that the total energy converged to within 1 meV/atom. Further details for the validation tests can be found elsewhere.[24]

The adsorption energy ΔE_{ads} is defined as

$$\Delta E_{ads}=E_{tot}-(E_{mol}+E_{sheet})$$

Where the E_{tot}, E_{mol} and E_{sheet} are the total energies of the adsorption complex, the isolated molecules and the GP/GO sheets, respectively.

The minimum energy pathway (MEP) from an initial state (IS) to its final state (FS) was determined by the nudged elastic band (NEB) method,[34,35] with 8-12 replicas interpolated. The

transition state (TS) was localized using the climbing image method and verified with single imaginary frequency. The convergence criterion was 0.02 eV/Å. It was estimated that the zero-point energy correction leads to a barrier decrease by 0.02 eV for the oxidation of SO_2 and 0.03 eV for NO. Spin polarization leads to barrier difference lower than 0.01 eV (see Table S1 and S2 in the supporting information). Therefore, it is acceptable for the ignorance of both of them.

3. Results

3.1 Oxidation of SO_2 to SO_3

3.1.1 Adsorption and oxidation on HO_OGP

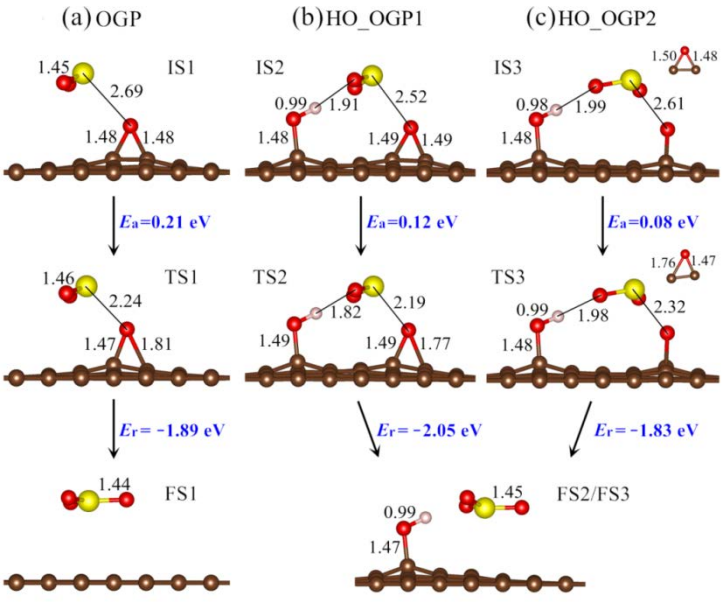

Figure 2 Minimum energy pathways (MEPs) for the oxidation of SO_2 by the epoxy group on (a) OGP, (b) HO_OGP1 and (c) HO_OGP2. The IS, TS and FS stand for initial, transitional and final states of the three reactions, respectively. The yellow ball represents the S atom. E_a is the activation energy, E_r is the reaction energy, defined as $E_{a/r} = E_{TS/FS} - E_{IS}$. Insets are included in (c) to show the geometry of the epoxy group. All the lengths are given in Å.

The MEP for the oxidation process SO_2/OGP → SO_3/GP is demonstrated as Figure 2a. On

SO_2 approaching the epoxy (from IS1 to TS1), the bond length of SO_2 is elongated from 1.45 to 1.46 Å, and is then converted to SO_3 with three equivalent bond lengths of 1.44 Å. Meanwhile, the oxygen atom of the epoxy group itself is drawn out of the GP surface from the two-foot bridge site to the single-foot top site. One O-C bond of the epoxy group is elongated by 0.33 Å and the other almost unchanged. The barrier and total energy release for the oxidation are 0.21 and 1.89 eV, respectively.

Table 1 Summary of adsorption energy, charge transfer and imaginary frequency validation for the adsorption and oxidation of SO_2, NO and CO on different GO surfaces.

Reactions	ΔE_{ads}, eV	Δq^*, e		f/i, cm^{-1}
	IS	IS	TS	TS
SO_2/OGP→SO_3/GP	–0.30	0.050	0.131	306
SO_2/HO_OGP1→SO_3/HO_GP	–0.40	0.060	0.141	194
SO_2/HO_OGP2→SO_3/HO_GP	–0.45	0.079	0.144	163
SO_2/2HO_OGP→SO_3/2HO_GP	–0.58	0.094	0.152	296
NO/OGP→NO_2/GP	–0.10	–0.051	–0.095	434
NO/HO_OGP1→NO_2/HO_GP	–0.54	0.005	–0.005	343
NO/HO_OGP2→NO_2/HO_GP	–0.25	–0.035	–0.086	301
CO/OGP→CO_2/GP	–0.09	0.003	0.004	450
CO/HO_OGP1→CO_2/HO_GP	–0.14	0.002	0.012	461
CO/HO_OGP2→CO_2/HO_GP	–0.15	0.007	0.005	471

*: The charge transfer Δq = Bader population – valence electrons, as a whole for an adsorbed molecule.

Figure 2b shows MEP for the oxidation of SO_2 on HO_OGP1 (see the topviews in Figure S1a in the supporting information). In the initial state IS2, the distance of the hydrogen bond H…O is 1.91 Å. The S-O distance is pulled much closer, from 2.69 in IS1 to 2.52 Å. In the TS2, the

hydrogen bond is shortened to 1.82 Å, while the on-breaking O-C bond of the epoxy group is elongated by 0.28 Å. The oxidation barrier is reduced to 0.12 eV, compared to 0.21 eV for the oxidation of SO_2 on OGP. Consequently, it can be assumed that the introduction of the hydroxyl group plays two roles: Enhancing the adsorption of SO_2 (see Table 1) and reducing the oxidation barrier. Nevertheless, based on further investigation as below, it does not tell the entire story.

Several other configurations of HO_OGP have been investigated and a more energetically favorable MEP for the oxidation of SO_2 is depicted in Figure 2c (see the topviews in Figure S1b in the supporting information). The adsorption of SO_2 on HO_GP2 is slightly preferable to HO_GP1 (see Table 1) and the oxidation barrier is reduced to 0.08 eV. However, compared to the configuration IS2, both distances of H…O (1.99 Å) and S-O (2.61 Å) are slightly longer, but non-negligible. In the TS3, the distance of H…O is 1.98 Å, almost unchanged. The S-O is reduced to 2.32 Å. Both of them are much longer than their counterparts in TS2. These differences indicate that the H-bonding interaction is not the only factor that enhances the adsorption and promotes the oxidation of SO_2 on the GO surface.

3.1.2 Adsorption and oxidation on 2HO_OGP

To further investigate the potential for the enhancement of the hydroxyl group on the oxidation of SO_2 on GO, a second hydroxyl group was added to HO_OGP to fabricate the 2HO_OGP configuration. The top and side views for the adsorption and oxidation of SO_2 on 2HO_OGP are shown in Figure 3. As expected, the adsorption energy of SO_2/2HO_OGP is increased to –0.58 eV. The oxidation barrier is further reduced to 0.06 eV. Two hydrogen bonds are formed between each of the two hydroxyl groups and the two oxygen atom of the adsorbed SO_2 molecule. In the

movie of the oxidation process, the two hydroxyl groups rotate according to the movement of SO_2, and keep pointing to each of the two oxygen atoms of the SO_2 molecule. The two bond lengths of the epoxy group in the IS configuration are 1.50-1.51 Å, which are the longest among those of SO_2/OGP and SO_2/HO_OGP. Meanwhile, the on-breaking O-C bond in TS is extended from 1.51 to 1.74 Å, by the lowest extent 0.23 Å.

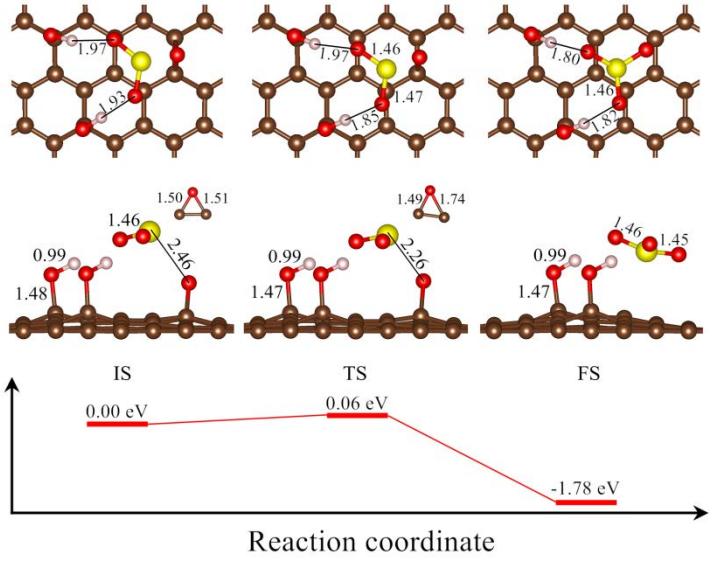

Figure 3 MEP for the oxidation of SO_2 by epoxy on 2HO_OGP. IS: SO_2/2HO_OGP; FS: SO_3/2HO_GP.

3.1.3 Charge transfer for adsorption and oxidation of SO_2

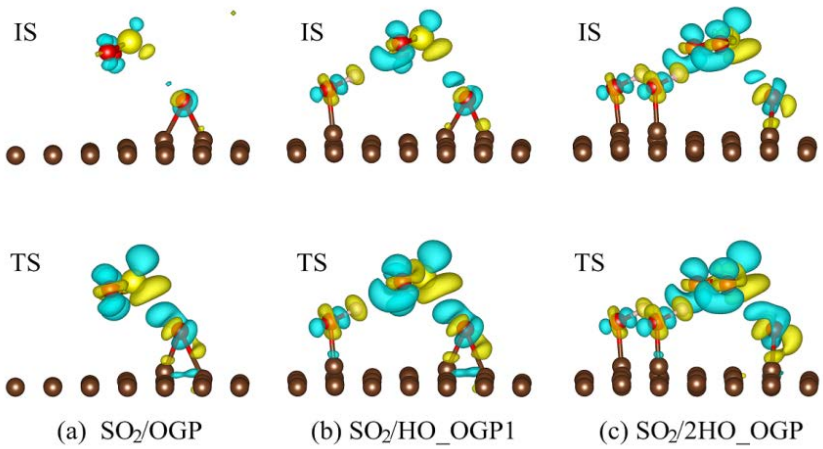

Figure 4 Charge differences for the initial state (IS) and transition state (TS) of SO_2 oxidation on

(a) OGP, (b) HO_OGP1 and (c) 2HO_OGP. All the isosurfaces are 0.02 e/Å^3. The blue (yellow) area denotes electron accumulation (depletion).

The promotion of the hydroxyl group to the adsorption and oxidation of SO_2 on GO surface has been ascribed to the strong hydrogen bonding interaction, which results in pre-activation of the epoxy group in the initial adsorption configuration.[24] Herein, both the charge transfer of the IS and TS configurations are of concern in order to give a more clear picture of the promotion mechanism.

Figure 4a shows the charge transfer pattern for the adsorption and oxidation of SO_2 on OGP. The IS in Figure 4a shows electrons are transferred in a back-donation way: (1) Electrons are transferred to the epoxy group, through the Coulomb interaction between the positive S(Ⅳ) atom and the negative O(-Ⅱ); and (2) electrons are transferred to the adsorbed SO_2 molecule through the π-π stacking interaction between the main graphene surface and the π_3^4 of SO_2. During the oxidation, more electrons are transferred to the adsorbed SO_2, and then to the epoxy, as both the blue and yellow areas increase, as shown in the TS. According to Bader population analysis (Table 1), in the IS configuration, the net charge transferred to the adsorbed SO_2 is 0.050e. It is increased to 0.131e in the TS configuration. The yellow area present at one of the O-C bonds of the epoxy group demonstrates the breaking.

The charge difference plots of SO_2/HO_OGP1 and SO_2/2HO_OGP are shown in Figure 4b and c, respectively. As the pattern of SO_2/HO_OGP2 is quite similar to SO_2/HO_OGP1, only the latter is presented here. The strong H-bonding interaction is confirmed in that there are considerable electron accumulated (blue) and depleted (yellow) areas on all the H…O bonds in

198 pairs. For SO_2/HO_OGP1, the net electron transfer to SO_2 is 0.060e in IS2 and 0.141e in TS2.
199 For SO_2/2HO_OGP, the two values are increased to 0.094e and 0.152e respectively. More
200 electrons are transferred from the two hydroxyl groups to the adsorbed SO_2 molecule in a
201 dual-channel manner. In summary, as listed in Table 1, for the adsorption and oxidation of SO_2 on
202 the four different GO surfaces, both the net charge transfers in the IS and TS configurations are
203 increased with increase of SO_2 adsorption energies. The oxidation barriers decrease
204 monotonically in the same order.

205 In Section 3.1.1, it has been mentioned that the hydrogen bond interaction for the adsorption
206 and oxidation of SO_2 on HO_OGP2 should be weaker than that on HO_OGP1. However, both the
207 adsorption energy and net charge transfers of the former are higher than those of the latter, and
208 with a lower oxidation barrier. It is due to the stronger π-π stacking interaction between the main
209 graphene surface and the π_3^4 of SO_2, since the topviews in Figure S1b for SO_2/HO_OGP2 show
210 the S-O bonds of the adsorbed SO_2 molecule are clearly parallel to the C-C bonds of the main GP
211 surface.

212 Consequently, the promotion of hydroxyl groups to the adsorption and oxidation of SO_2 on GO
213 surface can be ascribed to the unique charge transfer channels, through which electrons are
214 transferred from the hydroxyl group to the adsorbed SO_2, and in turn to the epoxy group. Through
215 the charge transfer channel, the epoxy group is not only pre-activated for further oxidation, but
216 also is well charged by SO_2 when climbing to the transitional state, which helps to reduce the
217 oxidation barrier intrinsically.

3.2 Oxidation of NO to NO_2

3.2.1 Adsorption and oxidation on OGP

The configuration for the adsorption of NO on OGP is shown as IS1 in Figure 5a. It is a typical weak physisorption since the adsorption energy is as low as –0.10 eV (Table 1), much lower than the value of –0.30 eV for SO_2/OGP. Additionally, the bond length of the adsorbed NO molecule remains the same as the calculated value of free NO, 1.17 Å. As shown in Figure 6a, electrons are transferred from NO to the OGP surface (0.051e). The charge transfer direction is opposite to that of SO_2. It has been explained[17,36] that the highest occupied molecule orbital (HOMO) of NO is higher than the Fermi level of OGP.

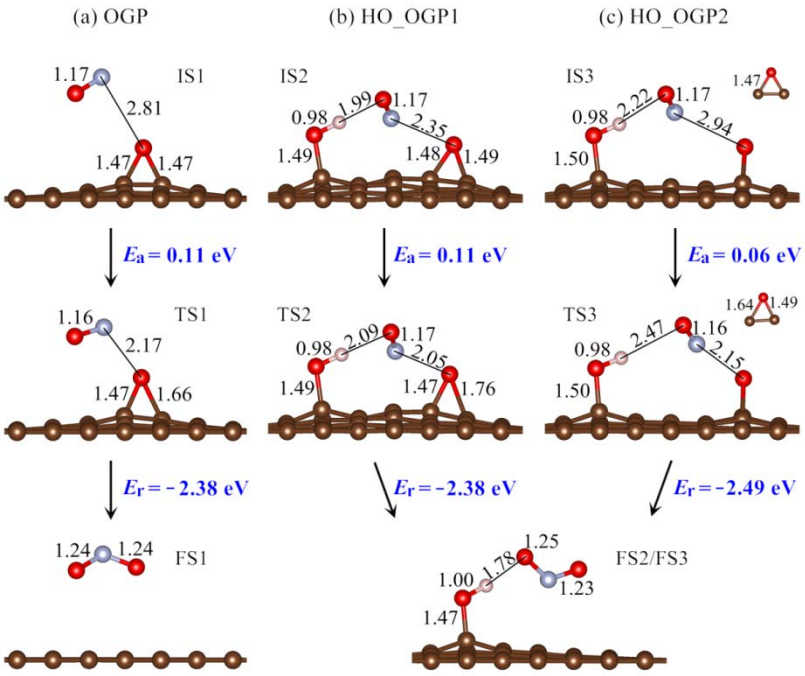

Figure 5 MEP for the oxidation of NO by the epoxy group on HO_OGP1 and HO_OGP2. Insets are included for HO_OGP2 to show the local geometry of the epoxy group in IS2 and TS2. IS1: NO/HO_OGP1; IS2: NO/HO_OGP2; FS: NO_2/HO_GP.

For the oxidation process NO/OGP → NO_2/GP (Figure 5a), the N-O bond of NO in TS1 is slightly shortened to 1.16 Å (it is 1.17 Å in IS1), rather than elongated to some extent. The

number of electrons donated by NO is increased to 0.095e. It is noteworthy that the oxidation barrier is 0.11 eV, which is about half of that for SO_2 on OGP. Such a low barrier indicates that NO can be oxidized by the epoxy group on OGP almost at room temperature. However, the prerequisite adsorption of NO on OGP is too weak to form an effective oxidation chain. It should be enhanced in some way.

3.2.2 Adsorption and oxidation on HO_OGP

The adsorption configurations NO/HO_OGP1 and NO/HO_OGP2 are shown as IS2 and IS3 in Figure 5b and c, respectively. Compared to the adsorbed configuration in NO/OGP, herein the NO is upside down, where the N atom is much closer to the GP surface than the O atom. In both situations, the adsorption of NO is well enhanced as the adsorption energy for NO/HO_OGP1 is –0.54 eV and that for NO/HO_OGP2 is –0.25 eV, compared to –0.11 eV for NO/OGP, likely due to the strong chemisorption for the adsorption of NO on HO_OGP.

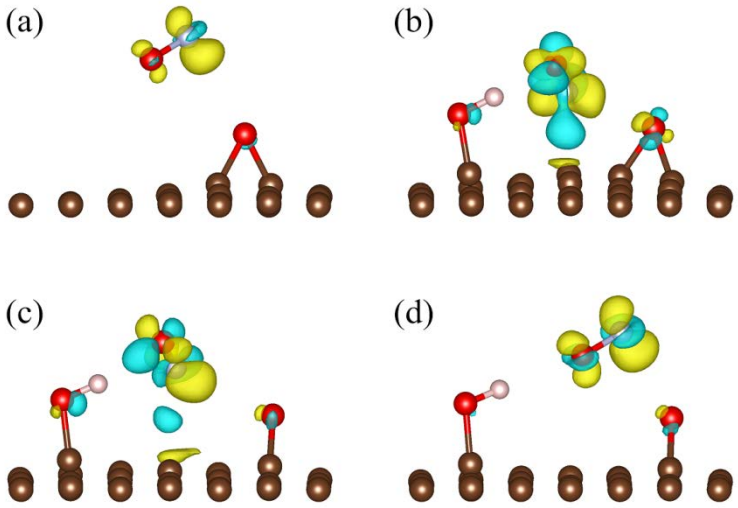

Figure 6 Charge difference plots for (a) NO/OGP, (b) NO/HO_OGP1, (c) NO/HO_OGP2 and (d) NO_d/HO_OGP2. The NO_d/HO_OGP2 is an alternative adsorbed configuration of NO on HO_OGP2, where the O atom is more close to the substrate than the N atom. The isosurface for

(b) is 0.03 e/Å^3, for others is 0.01 e/Å^3. Refer the configuration (d) and the oxidation related to Figure S3 in the supporting information.

The charge difference plots in Figure 6 help to explain the obvious difference in adsorption energy among NO/OGP, NO/HO_OGP1 and NO/HO_OGP2. As shown in Figure 6b for NO/HO_OGP1, there is a strong charge transfer from a C atom in the HO_OGP surface to the N atom of the adsorbed NO molecule. It results in a net charge transfer to the adsorbed NO molecule by 0.005 e, as listed in Table 1. A similar (but slightly weaker) electron transfer from the C atom to the N atom is shown in Figure 6c for NO/HO_OGP2, in which the donated electrons of the adsorbed NO are reduced from 0.051e to 0.035e. The strong covalent interaction between the adsorbed NO molecule and the HO_OGP surface makes it clear that NO is chemisorbed. Furthermore, there is weak hydrogen bonding interaction between the hydroxyl group and the adsorbed NO. The electron accumulation area around the O atom of NO is weakly polarized and is pointed towards the H atom of hydroxyl group.

The oxidation barrier for NO on HO_OGP1 is 0.11eV, equivalent to that for NO/OGP → NO_2/GP. However, for the oxidation of NO on HO_OGP2, the oxidation barrier is reduced to 0.06 eV, even lower than that for SO_2/HO_OGP2 (0.08 eV). When NO is adsorbed in the O down way (denoted as NO_d/HO_OGP2 in Figure 6d), the oxidation barrier is increased to 0.13 eV (see Figure S3 in the supporting information). It implies that the N-C covalent interaction helps to activate the NO molecule, and reduce the oxidation barrier.

It is now known that the oxidation barrier for the oxidation of NO by the epoxy group on GO is rather low. The introduction of the hydroxyl group can enhance the adsorption of NO, which in

turn facilitates the oxidation of NO by the epoxy groups of the GOs. It can also reduce the oxidation barrier, which depends on the relative locations of the epoxy groups to the hydroxyl groups.

3.3 Oxidation of CO to CO_2

3.3.1 Adsorption and oxidation on OGP

There is also a weak physisorption for CO on OGP in the IS1 configuration as shown in Figure 7a. The adsorption energy is –0.09 eV and the charge transfer is 0.003e to the adsorbed CO molecule (see Table 1). The bond length of the adsorbed CO molecule is 1.14 Å, remaining the same as that of a free CO molecule. The distance from the C atom of CO to the O atom of the epoxy group on the OGP surface is 2.95 Å, much longer than the value 2.81 Å for NO/OGP and 2.69 Å for SO_2/OGP.

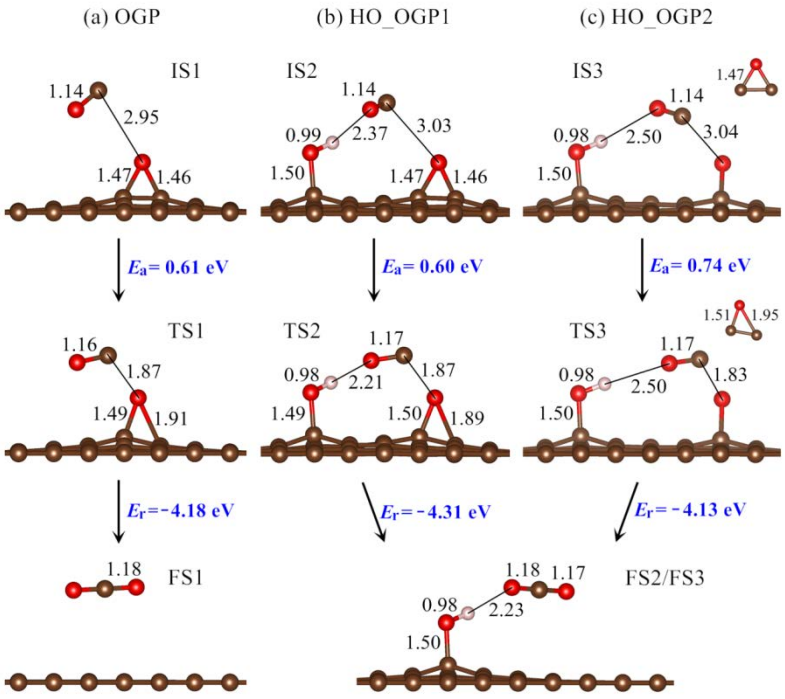

Figure 7 MEP for the oxidation of CO by the epoxy group on HO_OGP1 and HO_OGP2. Insets are included for HO_OGP2 to show the local geometry of the epoxy group in IS2 and TS2. IS1:

CO/HO_OGP1; IS2: CO/HO_OGP2; FS: CO2/HO_GP.

On CO approaching the epoxy group for the oxidation process CO/OGP → CO_2/GP (see Figure 7a), the bond length of CO is elongated from 1.14 to 1.16 Å, and then converted to CO_2 with two equivalent bond lengths of 1.18 Å. Meanwhile, the epoxy group itself is drawn out of the GP surface with the longest extended O-C bond length 1.91 Å, compared to 1.81 Å for SO_2/OGP and 1.66 Å for NO/OGP. The O-C distance is shorted from 2.95 to 1.87 Å. The calculated barrier for the oxidation is 0.61 eV (see Table 1), followed by an intensive energy release of 4.18 eV to form the final state CO_2/GP.

3.3.2 Adsorption and oxidation on HO_OGP

The adsorption configurations CO/HO_OGP1 and CO/HO_OGP2 are shown as IS2 and IS3 in Figure 7b and c, respectively. Insets are included for CO/HO_OGP2 to show the local geometries of the surface epoxy group. The introduction of the hydroxyl group seems to make little change to the weak physical adsorption process as the bond length of the adsorbed CO molecule remains 1.14 Å in both situations. The distances from the C atom of CO to the O atom of the epoxy group on the HO_OGP1 and HO_OGP2 surface are elongated slightly by *ca.* 0.1 Å (3.03 and 3.04 Å vs. 2.95 Å). The adsorption energy and charge transfer for CO/HO_OGP1 are –0.14 eV and 0.002 e, respectively; and for CO/HO_OGP2 are –0.15 eV and 0.007 e, respectively, as listed in Table 1. The two situations are similar, both energy-wise and geometrically.

The oxidation barrier for CO on HO_OGP1 is 0.60 eV, equivalent to 0.61 eV for CO/OGP → CO_2/GP. It is 0.74 eV for CO oxidation on HO_OGP2. The on-breaking O-C bond of the epoxy group is extended from 1.46 Å in IS2 to 1.89 Å in TS3, and from 1.47 Å in IS3 to 1.95 Å in TS3.

It seems that the oxidation barrier for CO on GOs depends on the extension of the epoxy group during the oxidation. When the oxidation barrier for CO oxidation is increased to the order 0.60 eV (HO_OGP1) < 0.61 eV (OGP) < 0.74 eV (HO_OGP2), the on-breaking O-C bond of the epoxy group is elongated by 0.43 Å (HO_OGP1) < 0.45 Å (OGP) < 0.48 Å (HO_OGP2). It implies that the activation of the surface epoxy is the key step for a surface oxidation process on GOs and the introduction of the hydroxyl group does not promote the oxidation of CO.

4. Discussion

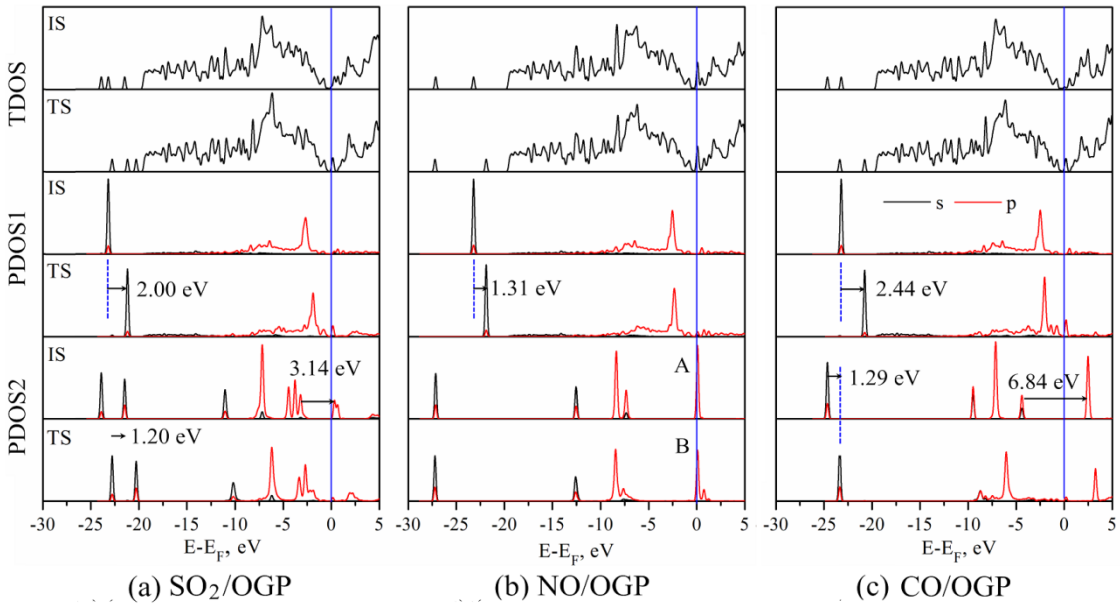

Figure 8 Density of states (DOS) analysis for the adsorption and oxidation of (a) SO_2, (b) NO and (c) CO on OGP surfaces. PDOS1 and PDOS2 stand for the projected density of states (PDOS) of the epoxy group and the adsorbed molecule, respectively.

It has been found that the oxidation of SO_2 and NO by epoxy groups on GO surfaces is kinetically preferable, and both the oxidation of SO_2 and NO can be promoted by the introduction of the hydroxyl group, which is not the case for CO. Herein, we focus on three points to make generalizations of our findings: (1) Why the capacities for the oxidation of SO_2, NO and CO by

epoxy groups on GO surface are different? (2) The relationship between the oxidation barrier and the activation of the epoxy group; and (3) the feasibility for the simultaneously catalytic removal of SO_2 and NO with well-prepared GOs.

As shown in Figure 8, during the oxidation from the IS to the TS configuration, the electronic structures of the epoxy group and the adsorbed molecules are changed. The variation of the oxidation barrier can be ascribed to the difference in the energy gap of the adsorbed molecules,[37] intrinsically, since electrons are activated from the highest occupied molecular orbit (HUMO) to the lowest unoccupied molecular orbit (LUMO) and then transferred to the epoxy group. The energy gap for SO_2/OGP is 3.14 eV (Figure 8a), and is a much narrower than the gap 6.84 eV for CO/OGP is (Figure 8c). Accordingly, the barrier is increased from 0.21 to 0.61 eV.

For the oxidation of NO on OGP (Figure 8b), there are partially occupied states just located at the Fermi level for both the IS (marked as A and see Figure S4 in the supporting information) and TS (marked as B) configuration of the adsorbed NO molecule. The intensity of state A is somewhat lower than that of B. Meanwhile, a new empty state is presents on the right of the latter. Other states at much lower energy levels are almost unchanged. These results indicate that the state at the Fermi level itself acts as an electron donor and acceptor, which results in a lowest oxidation barrier of 0.11 eV.

In Section 3.1, it is shown that the barrier for SO_2 oxidation on the four different GO surfaces is positively correlated to the extension of the on-breaking O-C bond of the epoxy group. The same trend is also found for the oxidation of CO (see Section 3.3). All the barriers and the corresponding extensions of the O-C bond are collected and dotted as shown in Figure 9. It can

be seen that, except for the two oxidations of NO on OGP (marked as A) and HO_OGP2 (marked as B), all the other points are uniformly dispersed around the trend line. It implies that more attention should be paid to the activation of the epoxy group on the GO surface for any potential application in catalytic oxidation.

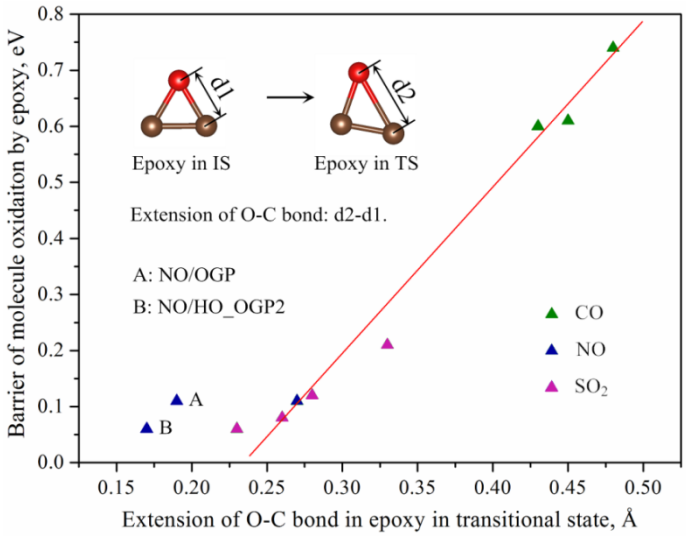

Figure 9 Dependence of the oxidation barrier for SO_2, NO and CO on the extension of the on-breaking O-C bond of the epoxy group. IS and TS represent the initial state and final state in an elementary oxidation process. The extension is shown in the inset.

In most cases, humidity is inevitable as a disturbing influence on the catalytic oxidation of SO_2 and NO from flue gases.[38-41] The calculated adsorption energy of a single H_2O molecule on HO_OGP1, HO_OGP2 and 2HO_OGP are –0.54, –0.55 and –0.73 eV, respectively. Each is thermodynamically preferable to the corresponding values for SO_2. The highest adsorption energy of NO (on HO_OGP1) is –0.54 eV, equivalent to the adsorption energy of H_2O on HO_OGP1 and HO_OGP2. Nevertheless, the concentration of NO in the gaseous phase is of the order 0.1 vol %, compared to 1 vol % for water. The adsorption of H_2O is still more preferable to NO. However, many experimental studies have confirmed that humidity can promote the

catalytic oxidation of SO_2,[42,43] while strongly inhibiting the catalytic oxidation of NO.[12] The opposite effects are likely due to the solubility difference of SO_2 and NO in water. Therefore, it seems unfeasible to have simultaneous removal of SO_2 and NO by catalytic oxidation on GOs, in the presence of water.

5. Conclusions

Density functional theory corrected with dispersion was used to investigate the mechanism for the oxidation of SO_2 and NO_x on graphene oxides. It was found that both SO_2 and NO_x could be oxidized by GO at near room temperature. Epoxy groups should be the active sites where SO_2 and NO molecules are oxidized. It is of more importance that hydroxyl groups can help to enhance the adsorption of the two species, and facilitate their oxidation by reducing the activation barrier. The promotion of the hydroxyl group for SO_2 is derived from the formation of charge transfer channels, which are fabricated by the hydroxyl group, the adsorbed SO_2 and the epoxy group. It can be enhanced by introduction of more hydroxyl groups as more charge transfer channels will be formed. However, for NO, the promotion is due to the strong N-C covalent interaction between the adsorbed NO molecule and the GO surface, through which the NO is activated and oxidized with much lower resistance. Further exploration is needed to determine the effects of humidity on the adsorption and oxidation of SO_2 and NO.

Acknowledgements

This work was financially supported by the National Nature Science Youth Fund of China (5110828) and the Department of Science and Technology of Sichuan Province in China

(2011HH0009). We also acknowledge the National Supercomputer Center in Shenzhen City of China for computational service support.

References

(1) Long, X. L.; Xin, Z. L.; Wang, H. X.; Xiao, W. D.; Yuan, W. K., Simultaneous Removal of NO and SO_2 with Hexamminecobalt(II) Solution Coupled with the Hexamminecobalt(II) Regeneration Catalyzed by Activated Carbon, *Appl. Catal. B-Environ.* **2004**, *54*, 25-32.

(2) Zeng, Z.; Lu, P.; Li, C.; Mai, L.; Li, Z.; Zhang, Y., Removal of NO by Carbonaceous Materials at Room Temperature: A Review, *Catal.Sci. Technol.* **2012**, *2*, 2188-2199.

(3) Mochida, I.; Korai, Y.; Shirahama, M.; Kawano, S.; Hada, T.; Seo, Y.; Yoshikawa, M.; Yasutake, A., Removal of SO_x and NO_x over Activated Carbon Fibers, *Carbon* **2000**, *38*, 227-239.

(4) Long, Y.; Zhang, C.; Wang, X.; Gao, J.; Wang, W.; Liu, Y., Oxidation of SO_2 to SO_3 Catalyzed by Graphene Oxide Foams, *J. Mater. Chem.* **2011**, *21*, 13934.

(5) Lee, J. K.; Juh, D. J.; Park, D.; Park, S., Sulfur-Dioxide Adsorption over Activated Lignite Char Prepared from Fluidized-Bed Pyrolysis, *Chem. Eng. Sci.* **1994**, *49*, 4483-4489.

(6) Lee, J. K.; Ferrero, S.; Hudgins, R. R.; Silveston, P. L., Catalytic SO_2 Oxidation in a Periodically Operated Trickle-Bed Reactor, *Can. J. Chem. Eng.* **1996**, *74*, 706-712.

(7) Lizzio, A. A.; DeBarr, J. A., Mechanism of SO_2 Removal by Carbon, *Energ. Fuel.* **1997**, *11*, 284-291.

(8) Li, Y. X.; Cheng, Z. M.; Liu, L. H.; Yuan, W. K., Catalytic Oxidation of Dilute SO_2 over Activated Carbon Coupled with Partial Liquid Phase Vaporization, *Chem. Eng. Sci.* **1999**, *54*, 1571-1576.

(9) Yang, F. H.; Yang, R. T., Ab Initio Molecular Orbital Study of the Mechanism of SO_2 Oxidation Catalyzed by Carbon, *Carbon* **2003**, *41*, 2149-2158.

(10) Liu, L. M.; Car, R.; Selloni, A.; Dabbs, D. M.; Aksay, I. A.; Yetter, R. A., Enhanced Thermal Decomposition of Nitromethane on Functionalized Graphene Sheets: Ab Initio Molecular Dynamics Simulations, *J. Am. Chem. Soc.* **2012**, *134*, 19011-19016.

(11) Adapa, S.; Gaur, V.; Verma, N., Catalytic Oxidation of NO by Activated Carbon Fiber (ACF), *Chem. Eng. J.* **2006**, *116*, 25-37.

(12) Guo, Z.; Xie, Y.; Hong, I.; Kim, J., Catalytic Oxidation of NO to NO_2 on Activated Carbon, *Energ. Convers. Manage.* **2001**, *42*, 2005-2018.

(13) Mochida, I.; Kawabuchi, Y.; Kawano, S.; Matsumura, Y.; Yoshikawa, M., High Catalytic Activity of Pitch Based Activated Carbon Fibres of Moderate Surface Area for Oxidation of NO to NO_2 at Room Temperature, *Fuel* **1997**, *76*, 543-548.

(14) Talukdar, P.; Bhaduri, B.; Verma, N., Catalytic Oxidation of NO over CNF/ACF-Supported CeO_2 and Cu Nanoparticles at Room Temperature, *Ind. Eng. Chem. Res.* **2014**, *53*, 12537-12547.

(15) Wang, M.-X.; Huang, Z.-H.; Shen, K.; Kang, F.; Liang, K., Catalytically Oxidation of NO into NO_2 at Room Temperature by Graphitized Porous Nanofibers, *Catal. Today.* **2013**, *201*, 109-114.

(16) Atkinson, J. D.; Zhang, Z.; Yan, Z.; Rood, M. J., Evolution and Impact of Acidic Oxygen Functional Groups on Activated Carbon Fiber Cloth During NO Oxidation, *Carbon* **2013**, *54*, 444-453.

(17) Tang, S.; Cao, Z., Adsorption of Nitrogen Oxides on Graphene and Graphene Oxides: Insights from Density Functional Calculations, *J. Chem. Phys.* **2011**, *134*, 044710.

(18) Radovic, L. R.; Suarez, A.; Vallejos-Burgos, F.; Sofo, J. O., Oxygen Migration on the Graphene Surface. 2. Thermochemistry of Basal-Plane Diffusion (Hopping), *Carbon* **2011**, *49*, 4226-4238.

(19) Radovic, L. R.; Silva-Tapia, A. B.; Vallejos-Burgos, F., Oxygen Migration on the Graphene Surface. 1. Origin of Epoxide Groups, *Carbon* **2011**, *49*, 4218-4225.

(20) Bao, X.; Nie, X.; Deak, D. v.; Biddinger, E. J.; Luo, W.; Asthagiri, A.; Ozkan, U. S.; Hadad, C. M., A First-Principles Study of the Role of Quanternay-N Doping on the Oxygen Reduction Reation Activity and Selectivity of Graphene Edge Sites, *Top. Catal.* **2013**, *56*, 1623-1633.

(21) Boukhvalov, D. W.; Son, Y. W.; Ruoff, R. S., Water Splitting over Graphene-Based Catalysts: Ab Initio Calculations, *ACS Catal.* **2014**, *4*, 2016-2021.

(22) Li, W.; Gao, Y.; Chen, W.; Tang, P.; Li, W.; Shi, Z.; Su, D.; Wang, J.; Ma, D., Catalytic Epoxidation Reaction over N-Containing sp^2 Carbon Catalysts, *ACS Catalysis* **2014**, *4*, 1261-1266.

(23) Sen, D.; Thapa, R.; Chattopadhyay, K. K., A First-Principles Investigation of Oxygen Reduction Reaction Catalysis Capabilities of as Decorated Defect Graphene, *Dalton T.* **2014**, *43*, 15038-15047.

(24) Zhang, H.; Cen, W.; Liu, J.; Guo, J.; Yin, H.; Ning, P., Adsorption and Oxidation of SO_2 by Graphene Oxides: A van der Waals Density Functional Theory Study *Appl. Surf. Sci.* **2015**, *324*, 61-67.

(25) Kresse, G.; Furthmuller, J., Efficient Iterative Schemes for Ab Initio Total-Energy Calculations Using a Plane-Wave Basis Set, *Phys.Rev. B* **1996**, *54*, 11169-11186.

(26) Kresse, G.; Furthmuller, J., Efficiency of Ab-Initio Total Energy Calculations for Metals and Semiconductors Using a Plane-Wave Basis Set, *Comput. Mater. Sci.* **1996**, *6*, 15-50.

(27) Perdew, J. P.; Burke, K.; Ernzerhof, M., Generalized Gradient Approximation Made Simple, *Phys. Rev. Lett.* **1996**, *77*, 3865-3868.

(28) Blochl, P. E., Projector Augmented-Wave Method, *Phys. Rev. B* **1994**, *50*, 17953-17979.

(29) Kresse, G.; Joubert, D., From Ultrasoft Pseudopotentials to the Projector Augmented-Wave Method, *Phys. Rev. B* **1999**, *59*, 1758-1775.

(30) Grimme, S., Semiempirical GGA-Type Density Functional Constructed with a Long-Range Dispersion Correction, *J. Comput. Chem.* **2006**, *27*, 1787-1799.

(31) Klimes, J.; Browler, D. R.; Michaelides, A., Van der Waals Density Functionals Applied to Solids, *Phys. Rev. B* **2011**, *83*, 195131.

(32) Hamada, I., Adsorption of Water on Graphene: A van Der Waals Density Functional Study, *Phys. Rev. B* **2012**, *86*, 195436.

(33) Lazar, P.; Karlický, F.; Jurečka, P.; Kocman, M.; Otyepková, E.; Šafářová, K.; Otyepka, M., Adsorption of Small Organic Molecules on Graphene, *J. Am. Chem. Soc.* **2013**, *135*, 6372-6377.

(34) Henkelman, G.; Jonsson, H., Improved Tangent Estimate in the Nudged Elastic Band Method for Finding Minimum Energy Paths and Saddle Points, *J. Chem. Phys.* **2000**, *113*, 9978-9985.

(35) Henkelman, G.; Uberuaga, B. P.; Jonsson, H., A Climbing Image Nudged Elastic Band Method for Finding Saddle Points and Minimum Energy Paths, *J. Chem. Phys.* **2000**, *113*, 9901-9904.

(36) Leenaerts, O.; Partoens, B.; Peeters, F. M., Adsorption of H_2O, NH_3, CO, NO_2, and NO on Graphene: A First-Principles Study, *Phys. Rev. B* **2008**, *77*, 125416.

(37) Cen, W.; Liu, Y.; Wu, Z.; Wang, H.; Weng, X., A Theoretic Insight into the Catalytic Activity Promotion of CeO_2 Surfaces by Mn Doping, *Phys. Chem. Chem. Phys.* **2012**, *14*, 5769-5777.

(38) Yao, F.; Duong, D. L.; Lim, S. C.; Yang, S. B.; Hwang, H. R.; Yu, W. J.; Lee, I. H.; Güneş, F.; Lee, Y. H., Humidity-Assisted Selective Reactivity between NO_2 and SO_2 Gas on Carbon Nanotubes, *J.Mater. Chem.* **2011**, *21*, 4502.

(39) Garcia-Bordeje, E.; Pinilla, J. L.; Lazaro, M. J.; Moliner, R., NH_3-SCR of NO at Low Temperatures over Sulphated Vanadia on Carbon-Coated Monoliths: Effect of H_2O and SO_2 Traces in the Gas Feed, *Appl. Catal. B-Environ.* **2006**, *66*, 281-287.

(40) Lei, Z.; Han, B.; Yang, K.; Chen, B., Influence of H_2O on the Low-Temperature NH_3-SCR of NO over V_2O_5/AC Catalyst: An Experimental and Modeling Study, *Chem. Eng. J.* **2013**, *215*, 651-657.

(41) Liu, Y.; Yao, W.; Cao, X.; Weng, X.; Wang, Y.; Wang, H.; Wu, Z., Supercritical Water Syntheses of Ce_xTiO_2 Nano-Catalysts with a Strong Metal-Support Interaction for Selective Catalytic Reduction of NO with NH_3, *Appl. Catal. B-Environ.* **2014**, *160*, 684-691.

(42) Gaur, V.; Asthana, R.; Verma, N., Removal of SO_2 by Activated Carbon Fibers in the Presence of O_2 and H_2O, *Carbon* **2006**, *44*, 46-60.

(43) Guo, J.-x.; Liang, J.; Chu, Y.-H.; Sun, M.-C.; Yin, H.-Q.; Li, J.-J., Desulfurization Activity of Nickel Supported on Acid-Treated Activated Carbons, *Appl. Catal. A-Gen.* **2012**, *421*, 142-147.